

## Article

# Study on the Ageing Characteristics of Silicone Rubber for Composite Insulators under Multi-Factor Coupling Effects

Xinran Li <sup>1</sup>, Yuming Zhang <sup>2,\*</sup>, Lincong Chen <sup>1</sup>, Xiaotao Fu <sup>1</sup>, Jianghai Geng <sup>2</sup>, Yunpeng Liu <sup>2</sup> , Yijing Gong <sup>2</sup> and Simin Zhang <sup>2</sup>

<sup>1</sup> Key Laboratory of Physical and Chemical Analysis for Electric Power of Hainan Province, Hainan Power Grid Co., Ltd., Electric Power Research Institute, Haikou 570125, China; lxinran0513@163.com (X.L.); lyu1102@126.com (L.C.); xnxcz112@88.com (X.F.)

<sup>2</sup> Hebei Key Laboratory of Power Transmission Equipment Security Defense, North China Electric Power University, Baoding 071003, China; gengjh@ncepu.edu.cn (J.G.); liuyunpeng@ncepu.edu.cn (Y.L.); 220212213242@ncepu.edu.cn (Y.G.); 220192213164@ncepu.edu.cn (S.Z.)

\* Correspondence: 120222101036@ncepu.edu.cn

**Abstract:** Due to long-term exposure to high electrical field strength, heavy loads, and the complex climatic conditions in tropical coastal areas of China, widespread abnormal heating phenomena often occur in the operation of composite insulators in power transmission lines, posing a threat to the safe and stable operation of the power system. To study the ageing process of the silicone rubber sheath of composite insulators in the high-field, high-humidity, high-temperature, and high-salt-density environments along the coastal regions, this paper establishes a humidity–heat–electricity–salt spray accelerated ageing test platform and conducts ageing tests on silicone rubber materials for composite insulators under the coupled effect of multiple factors. The ageing characteristics of silicone rubber materials are analyzed using scanning electron microscopy, Fourier infrared spectroscopy, thermogravimetric analysis, and other methods. The results show that the coupled ageing factors have an impact on the surface morphology of silicone rubber. The continuous depolymerization of PDMS molecular chains leads to a decrease in the content of groups related to the hydrophobicity of the material, resulting in a deterioration of its hydrophobicity. Moreover, the degradation of silicone rubber materials and the enhanced moisture absorption capacity lead to an increase in the dielectric loss tangent of the saturated moisture-absorbing medium, thereby causing abnormal heating of the sheath at the end of the composite insulator. The research findings of this study are of significant reference value for revealing the degradation mechanism of composite insulator silicone rubber sheaths in tropical island environments and improving the service life of composite insulators.

**Keywords:** tropical coastal area; composite insulator; silicone rubber; ageing characteristic



**Citation:** Li, X.; Zhang, Y.; Chen, L.; Fu, X.; Geng, J.; Liu, Y.; Gong, Y.; Zhang, S. Study on the Ageing Characteristics of Silicone Rubber for Composite Insulators under Multi-Factor Coupling Effects. *Coatings* **2023**, *13*, 1668. <https://doi.org/10.3390/coatings13101668>

Academic Editor: Alicia de Andrés

Received: 20 August 2023

Revised: 13 September 2023

Accepted: 20 September 2023

Published: 23 September 2023



**Copyright:** © 2023 by the authors. Licensee MDPI, Basel, Switzerland. This article is an open access article distributed under the terms and conditions of the Creative Commons Attribution (CC BY) license (<https://creativecommons.org/licenses/by/4.0/>).

## 1. Introduction

With the implementation of China’s “marine strategy”, the strategic significance of coastal areas is increasingly prominent, and the construction of key infrastructure for smart grids is accelerating [1–4]. Hainan Province is located at the southernmost tip of China, surrounded by the sea. It is the only province in China with a tropical monsoon maritime climate, characterized by high temperatures, high humidity, high irradiation and high salt content [5]. It possesses unique and distinctive climatic characteristics nationwide. Composite insulators account for 80% of the total number of insulators in the power transmission lines of the Hainan power grid. In recent years, there has been widespread occurrence of abnormal heating in the operation of composite insulators on transmission lines due to long-term exposure to high electric field intensity, heavy loads, and complex weather conditions. After the degradation of the outer sheath of some composite insulators reaches a certain extent, signs of degradation also appear in the internal core rods. This poses a threat to the safe and stable operation of the power system. However, there is

currently limited research on the aging process and characteristics of silicone rubber used in composite insulators under the typical tropical island climate of Hainan Island. It is therefore urgent to supplement relevant studies in this area [6–8].

Composite insulators are composed of GFRP (glass fiber-reinforced plastic) core rods and an external silicone rubber sheath. The core rod primarily provides electrical insulation and mechanical load-bearing functions, while the external silicone rubber sheath protects the core rod. Specifically, the silicone rubber sheath effectively prevents external moisture, dust, and chemical substances from corroding the insulator core. It exhibits high dielectric strength and insulation performance, effectively isolating the electric field between the insulator core rod and the external environment, thus avoiding electrical failures and improving the service life and reliability of the insulator. However, due to prolonged exposure to high electric field intensity, high temperatures, high humidity, high salt spray, and other complex external environments, aging is inevitable [9–16]. Some research has been conducted on the aging characteristics of silicone rubber materials. Cheng Li et al., conducted extraction and testing research on composite insulators that have been in operation for many years and found that the electrical and mechanical performance of the silicone rubber sheath of composite insulators gradually decreases with the increasing duration of operation [17]. Li Shuzhen et al. have developed a silicone rubber aging test method that takes into account temperature cycling. They have summarized the effects of temperature cycling on the aging mechanism and behavior of silicone rubber, and confirmed that temperature cycling can lead to the fatigue failure of silicone rubber material [18]. Zhang Zhongyuan et al. utilized scanning electron microscopy and Fourier transform infrared spectroscopy to analyze the degradation mechanism of the silicone rubber sheath on the surface of composite crossarms under the individual effects of different aging factors. They found that the insulation performance of silicone rubber decreased to varying degrees after aging [19]. Zhang Zhijin et al. conducted ageing experiments on silicone rubber samples under a salt spray environment, and the results showed that the dielectric strength and physical and chemical properties of the material were all reduced [20]. Liang Ying et al. analyzed the effects of three individual aging factors, namely corona voltage, exposure time, nitric acid, and humidity, on the aging characteristics of silicone rubber materials in composite insulators. They pointed out that during the corona discharge process, charged particles bombard the silicone rubber material, resulting in degradation of its surface morphology, hydrophobicity, and trap characteristics [21].

In summary, previous research has mainly focused on the aging mechanism and performance degradation of silicone rubber sheath materials in composite insulators under the influence of individual aging factors. There has been less attention given to the aging characteristics of composite insulators under the combined effects of multiple factors, and there have only been occasional studies that consider the aging test with two or more aging factors. In particular, there is a lack of experimental research and relevant data on the aging process and characteristic behaviors of silicone rubber materials used in composite insulators under the typical climate conditions of high field strength, high temperature, high humidity, and high salt spray in tropical coastal areas.

In response to the deficiencies identified in the previous studies mentioned above, this paper established a humidity–heat–electricity–salt spray accelerated ageing test platform to carry out ageing tests on composite insulators under the combined action of high temperature, high humidity, high salt spray, and high field strength in typical tropical coastal regions. The saturation moisture absorption rate and dielectric parameters of silicone rubber specimens with different ageing durations were tested, and the ageing characteristics of silicone rubber materials under the combined ageing of multiple factors were studied by using scanning electron microscopy, Fourier transform infrared spectroscopy and thermogravimetric analysis. The aim is to provide a theoretical basis for the safe use of composite insulators by power grid companies and to improve the operational reliability of composite insulators in the high-field strength, high-temperature, high-humidity, and high-salt spray environments of tropical coastal regions.

## 2. Materials and Methods

### 2.1. Samples

The silicone rubber sample selected for the experiment is a high-temperature vulcanized silicone rubber sheet made of the same material as the sheath of composite insulators [22]. It was prepared by using methyl vinyl silicone rubber as the raw rubber, which is copolymerized with a small amount of vinyl silicone oil, with a vinyl content generally around 0.2% (molar fraction), and adding main additives such as flame retardants (aluminium hydroxide ATH) with good resistance to electrical erosion and thermal conductivity, reinforcing agents (white carbon black  $\text{SiO}_2$ ) that can improve mechanical strength, colourants, and peroxide curing agents. The curing process takes place at 135 °C for 10 min. The composition of the formulation includes 100 parts per hundred rubber (phr) of raw rubber, 80 phr of flame retardant, and 30 phr of reinforcing filler. The detailed mass ratio is shown in Table 1. The specific production process is as follows. First, silicone oil, gas-phase white carbon black, and aluminum hydroxide are fully mixed in a mixer to make a compounding rubber. Then, the compounding rubber is vulcanized into silicone rubber sheets in a mold with dimensions of 320 mm × 300 mm × 2 mm. The vulcanizing agent used is a peroxide with a vulcanization temperature of 135 °C and a vulcanization time of 12 min. Finally, a hydraulic press and a mold knife are used to cut the silicone rubber sheets into square pieces with a thickness of 2 mm, which are then stored at room temperature in the air for later use.

**Table 1.** Compounding formulation of silicone rubber material.

Compounding Formulation	Silicone Rubber	ATH	$\text{SiO}_2$	$\text{Fe}_2\text{O}_3$	$\text{C}_{10}\text{H}_{22}$	Hydroxyethyl-Silicone Oil
Mass ratio (phr)	100	80	30	5	3	5

As shown in Figure 1, square test specimens with a thickness of 2 mm are cut into circular samples with a diameter of 30 mm for ageing tests in conjunction with the needle plate electrodes. Before the aging test, the silicone rubber samples are thoroughly wiped with an alcohol solution to avoid interference from other factors on the test results. Afterwards, the samples are placed in an indoor environment for the alcohol to evaporate completely before being used.

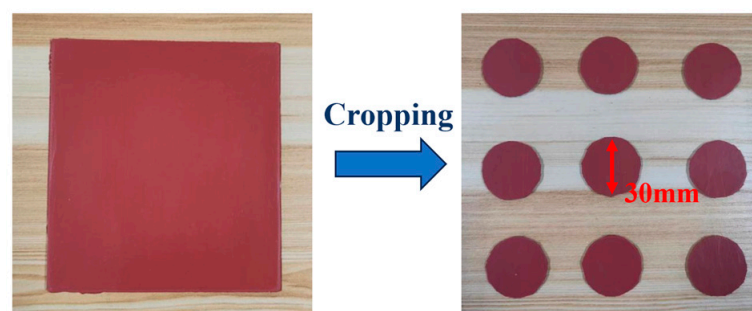


**Figure 1.** Preparation of silicone rubber samples.

### 2.2. Experimental Setup

#### 2.2.1. Humidity–Heat–Electricity Ageing Test Platform

As shown in the diagram, the humidity–heat ageing chamber utilizes the high- and low-temperature alternating damp heat test chamber produced by Dongguan Pengrui Testing Equipment Co., Ltd. (Dongguan, China) The temperature range within the test chamber is controllable from −20 °C to +150 °C, and the humidity range is from 20% to 98% RH. Additionally, a high-voltage bushing is installed on the upper wall of the high- and low-temperature alternating damp heat test chamber to allow the high-voltage power

line to enter the chamber. This is used to apply power frequency voltage to the needle plate electrodes inside the chamber, simulating the ageing environment of silicone rubber under high electric field conditions. The overall structure of the humidity–heat–electricity ageing test platform is shown in Figure 2.

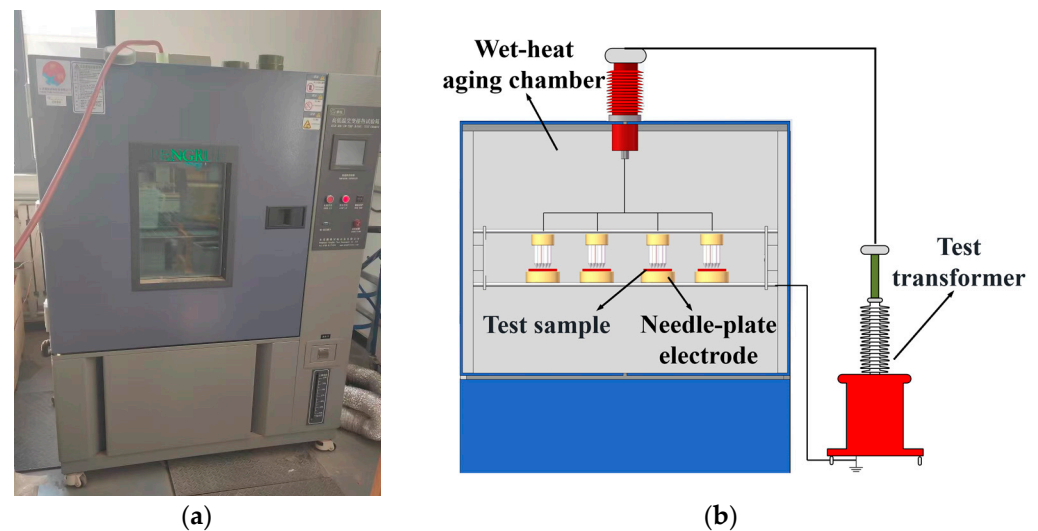
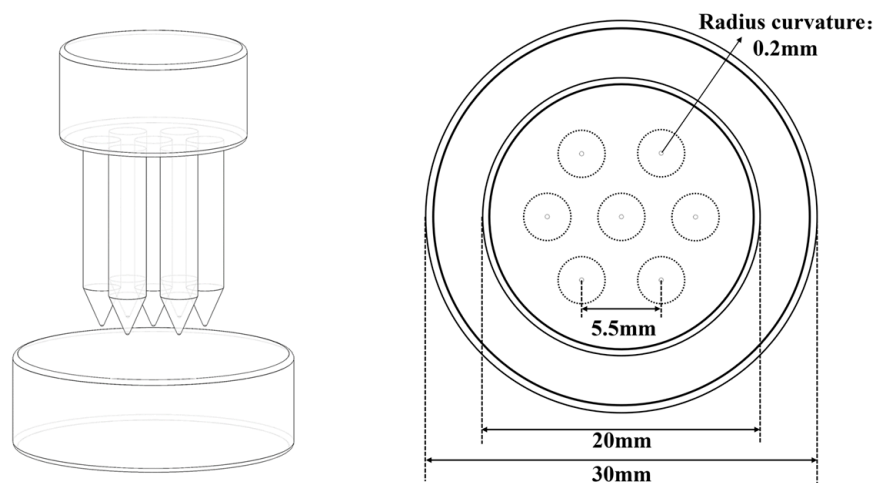


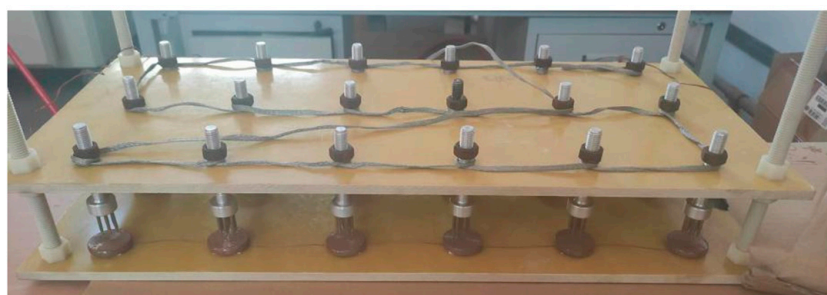
**Figure 2.** Humidity–heat–electricity ageing test platform. (a) Appearance; (b) schematic diagram.

The needle electrode in the needle–plate electrode configuration is a multi-needle structure. The electrode base has a diameter of 20 mm, and the curvature radius at the needle tip is 0.2 mm. The distance between the needles is 5.5 mm. There are a total of seven needles on one needle electrode, with one needle at the centre and the other six evenly distributed in the shape of a regular hexagon. The plate electrode is the lower electrode with a diameter of 30 mm, and it is grounded via a shielded cable. The electrode system of the corona withstand voltage test device includes a total of 18 sets of needle–plate electrodes arranged in a  $6 \times 3$  grid, with a distance of 90 mm between each set of needle–plate electrodes. The needle electrode base is connected to the threaded rod, allowing the distance between the needle electrode and the plate electrode to be adjusted by rotating the threaded rod. The schematic diagram of the needle–plate electrode is shown in Figure 3.

Before designing the electrodes for the experimental setup in this study, the maximum electric field intensity on the surface of the composite insulator sheath was simulated and calculated using finite element simulation. The simulation results are shown in Figure 4a. From Figure 4a, it can be seen that the maximum field strength on the surface of the 220 kV composite insulator without equipping grading rings reaches 1552.24 V/m. Therefore, in designing the electrodes in this study, it is desirable to apply an electric field strength of approximately 1600 V/m on the surface of the silicone rubber material in order to simulate the extreme electric field strength experienced in actual operation. When the distance between the needle tip and the ground electrode is 3 mm and a power frequency voltage of 6 kV is applied to the high-voltage electrode, the peak electric field strength between the needle electrode and the ground electrode is equivalent to the maximum surface field strength of the composite insulator sheath under extreme conditions. The surface electric field distribution on the silicone rubber sample is shown in Figure 4b. Additionally, a certain distance is maintained between the needles in order to prevent excessive concentration of the electric field, which could lead to premature breakdown of the silicone rubber test specimens.

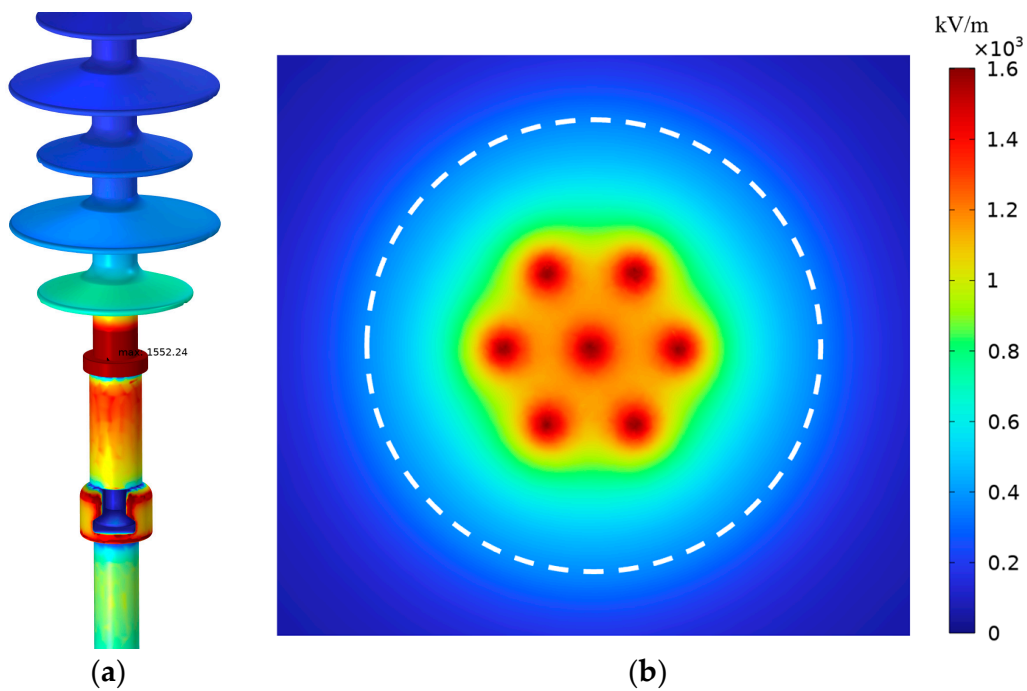


(a)



(b)

Figure 3. Needle-plate electrode. (a) Schematic diagram and dimensions; (b) arrangement.



(a)

(b)

Figure 4. The distribution of the surface electric field on composite insulators and the application of the electric field on needle plate electrodes. (a) The distribution of electric fields on the surface of the composite insulator; (b) distribution of electric field strength for the needle-plate electrode.



### 2.2.2. Salt Spray Ageing Test Platform

The salt spray ageing test platform uses a 90-type programmable salt spray test machine. The material of the test machine's box is a rigid PVC plastic board, and the box cover is made of transparent PVC board for easy observation. The salt spray deposition rate of the test machine is 1.0–2.0 mL/80 cm<sup>2</sup>·h. The nozzle is a PYREX glass precision nozzle, and its appearance is shown in Figure 5.



**Figure 5.** Salt spray ageing test platform.

### 2.3. Aging Conditions

The artificial ageing test conditions reference the climate environment of Haikou City, Hainan Province, China. This region is located south of the Tropic of Cancer and north of the Equator, between 19°32′–20°05′ N latitude and 110°10′–110°41′ E longitude. It is situated on the northern edge of the low-latitude tropical zone and has a tropical maritime monsoon climate. The annual average temperature is 24.2 °C, with the highest average temperature at around 28 °C and an extreme temperature of 39.6 °C. The air is humid, with an average relative humidity of 86% RH.

Based on this, the test conditions for the high- and low-temperature alternating humidity test chamber are set at a test temperature of 40 °C ± 2 °C and a relative humidity of 93% ± 3% RH. The salt spray accelerated ageing test is conducted according to GB/T 2423.17-2008 [23]. To better simulate the marine atmospheric environment, a neutral salt spray environment is used. The test solution is prepared by dissolving 50 g of NaCl in 1 L of deionized water. The temperature in the test chamber is set at a constant 35 °C, and the relative humidity at the nozzle should be at least 85%.

As shown in Table 2, this study divides the single-cycle multi-factor ageing test into two stages: 0–24 h and 25–48 h. During the 0–24 h period, the silicone rubber test samples undergo a humidity–heat–electricity corona ageing test. During the 25–48 h period, the silicone rubber test samples undergo a salt spray ageing test. After the tests, the test specimens' surfaces are thoroughly cleaned to remove salt residue that may affect the next cycle of ageing tests or subsequent performance testing. The total duration of the multi-factor ageing test is 32 days, spanning 16 cycles.

**Table 2.** Multi-factor ageing test plan.

Ageing Factor	Condition Parameter	Ageing Stages	
		0~24 h	25~48 h
voltage	AC 14 kv	√	--
humidity	(95 ± 3) %	√	--
temperature	(40 ± 2) °C	√	--
salt spray	NaCl: 50.0 kg/m <sup>3</sup>	--	√

## 2.4. Testing and Characterization

### 2.4.1. Scanning Electron Microscopy (SEM) Testing

FEI NOVA NANO450 field emission scanning electron microscopy was used to perform the microscopic morphology analysis on silicon rubber samples at different aging stages to study the surface morphology changes of silicon rubber.

### 2.4.2. Fourier Transform Infrared (FTIR) Spectrum Analysis

An IRTracer-100 Fourier transform infrared spectrometer was used to perform attenuated total reflection (ATR) scanning tests on silicon rubber samples at different aging stages. The differences in functional group content before and after aging were obtained based on the different peak absorbance values of the infrared characteristic peaks of the functional groups.

### 2.4.3. Thermogravimetric Analysis (TGA)

A PerkinElmer STA6000 thermogravimetric analyzer was used to perform thermal weight loss analysis on silicon rubber samples at different aging stages in order to study the thermal decomposition characteristics of silicon rubber materials before and after aging. The testing temperature range was 30 °C to 800 °C with a heating rate of 10 °C/min, and the protective gas used was nitrogen.

### 2.4.4. Moisture Absorption Test

To study the effect of multi-factor joint ageing tests on the moisture absorption characteristics of silicone rubber, the moisture absorption weight gain test of silicone rubber samples was conducted according to ASTM D5229 standard [24]. The equipment used for the moisture absorption weight gain test includes the SN-HWS-30B constant temperature and humidity test chamber produced by Shanghai Shangyi Instrument Equipment Co., Ltd. (Shanghai, China), and the FA224C electronic analytical balance produced by Shanghai Lichen Instrument Technology Co., Ltd. (Shanghai, China), with a measurement accuracy of 0.1 mg.

First, the samples were placed in a 50 °C oven until the sample mass reached a constant value in order to remove the initial moisture from the samples. The test temperature and humidity were set at 30 °C/90% RH. Three replicate samples were tested for each group, and the samples were periodically taken out from the constant temperature and humidity test chamber for weighing. The weighing results were averaged for the three samples. Before weighing the samples, any residual moisture on the sample surface was wiped clean. After weighing, the samples were quickly placed back into the test chamber for continued moisture absorption testing. This process was repeated until the sample weight no longer changed, indicating the saturation moisture absorption level. The moisture absorption rate  $M_t$  was calculated for each sample at time  $t$  as the weight difference between the initial weight  $W_0$  and the weight  $W_t$  at time  $t$ , according to Equation (1) [25].

$$M_t = \frac{W_t - W_0}{W_0} \times 100\% \quad (1)$$

### 2.4.5. Dielectric Loss Characteristic

The dielectric loss tangent of silicone rubber circular specimens in a saturated moisture absorption state was tested using a Nove-control broadband dielectric impedance spectroscopy instrument with a testing time not exceeding 2 min. The dielectric loss tangent value at a frequency of 50 Hz for the silicone rubber specimens in the saturated moisture absorption state is the average value of three specimen losses.

## 3. Results and Analysis

### 3.1. Appearance and Surface Morphology

The surface morphology and scanning electron microscopy (SEM) test results of silicone rubber specimens after different ageing durations are shown in Figure 6. From the figure, it can be observed that the surface of the silicone rubber specimen without corona ageing is smooth and glossy with a dense structure. As the ageing time increases, circular diffusion ageing areas appear on the surface of the specimen just below the needle tip, accompanied by the precipitation of greyish-white powdery substances. SEM images reveal that the surface of the specimen becomes rough, with localized fragmentation and the presence of filler particle precipitation. After 16 cycles of ageing, the circular diffusion ageing area further expands, and the accumulation of greyish-white powdery substances becomes severe. Cracks on the surface of the specimen deepen in the SEM images, and deep holes appear in multiple locations, indicating further degradation.

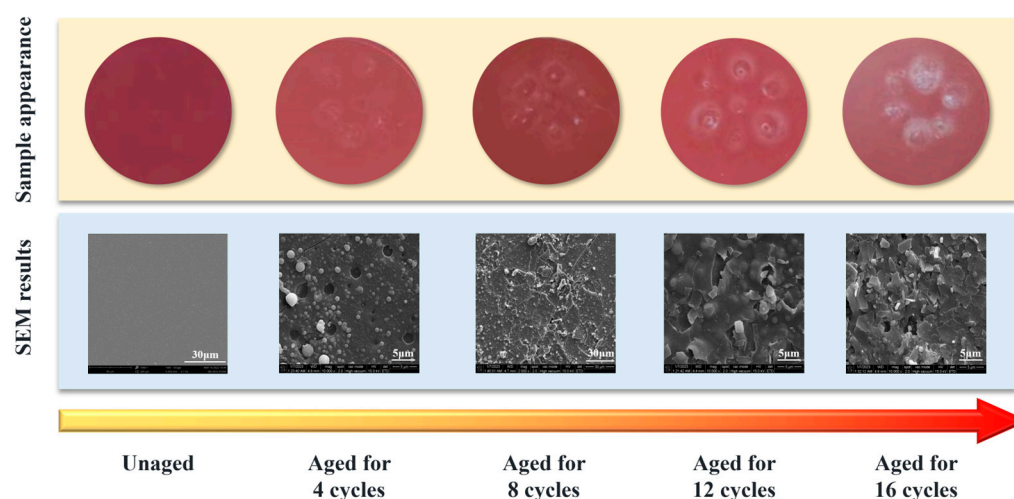


**Figure 6.** Changes in the appearance and surface morphology of the samples.

### 3.2. Fourier Transform Infrared Spectroscopy Analysis

The main component of the silicone rubber used in composite insulators is polydimethylsiloxane (PDMS). The Si–O–Si on the main chain and the Si–CH<sub>3</sub> on the side chain ensure the hydrophobic properties of the silicone rubber material [26]. The wavelength range of the main functional groups and corresponding characteristic absorption peaks in the silicone rubber used for composite insulators are shown in Table 3.

**Table 3.** The wavelength range of characteristic absorption peaks.

Characteristic Functional Group	Wavenumbers/cm <sup>-1</sup>	Mode of Vibration
O–H	3700–3200	stretching
(C–H) in CH <sub>3</sub>	2960	stretching
(C–H) in Si–CH <sub>3</sub>	1270–1255	bending
(Si–O) in Si–O–Si	1100–1000	stretching
Si–(CH <sub>3</sub> ) <sub>2</sub>	840–790	stretching



Based on the FTIR test results of samples with different ageing periods in Figure 7, it can be observed that, compared to the new samples, no new characteristic peaks are appearing and no existing characteristic peaks are disappearing in the samples with different ageing periods. This indicates that there is no formation of new substances or complete disappearance of components in the silicone rubber material during the artificial accelerated aging test. As the ageing period increases, the absorbance of the Si–O–Si groups in the  $1000\text{ cm}^{-1}$  to  $1100\text{ cm}^{-1}$  wavelength range gradually decreases. This suggests that a significant amount of energy released during the corona ageing process continues to act on the PDMS molecular chain, causing continuous chain scission. The reaction equation is shown in Figure 8, resulting in the formation of smaller molecular chains with different functional groups and free hydroxyl groups.

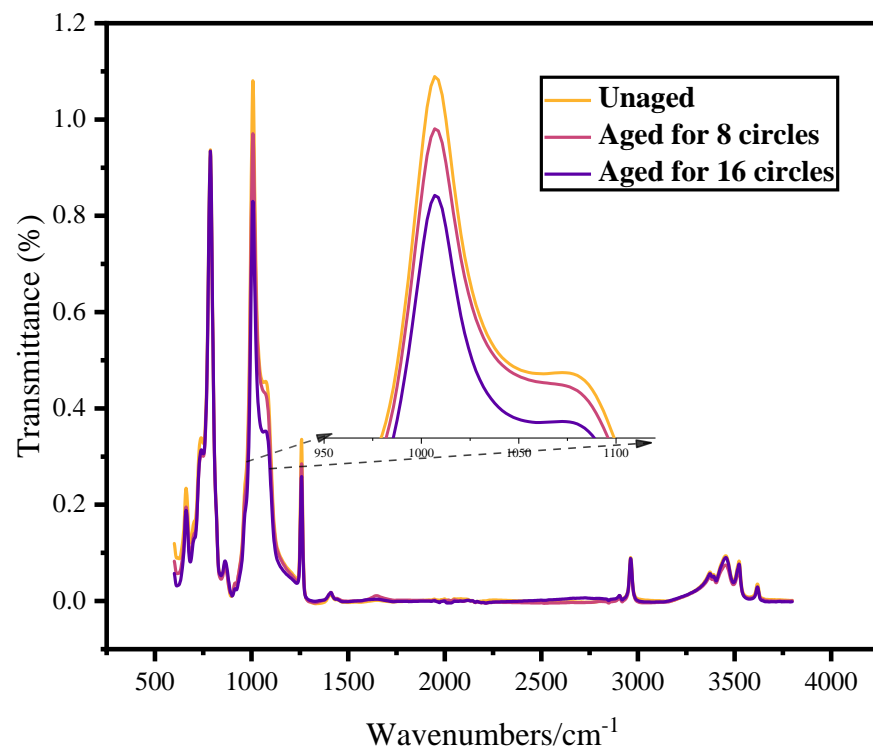


Figure 7. FTIR test results of samples with different ageing periods.

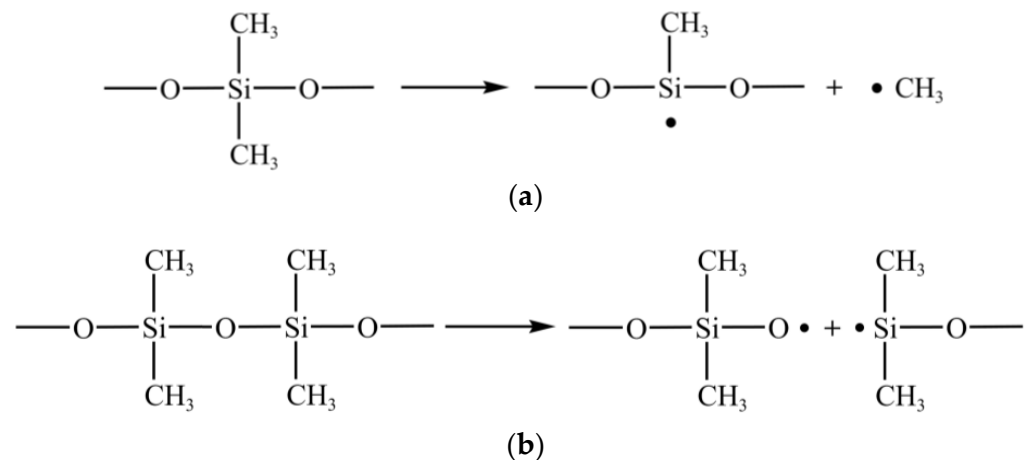


Figure 8. Reaction equation for the cleavage of the PDMS main chain. (a) Reaction 1; (b) Reaction 2.

### 3.3. Thermogravimetric Analysis

To further confirm that corona ageing causes PDMS degradation, this study also conducted thermogravimetric analysis (TGA) on silicone rubber samples at different ageing stages. The composite insulator is composed of silicone rubber, which consists of polydimethylsiloxane (PDMS), flame retardant alumina trihydrate (ATH), and fumed silica. Due to the high melting point of fumed silica at approximately 1600 °C, which is much higher than the maximum experimental temperature of 800 °C, fumed silica does not decompose during the TGA experiment. The weight loss of the samples is mainly attributed to the dehydration and decomposition of ATH and PDMS. The thermal decomposition process can be divided into two stages, with ATH decomposing in the temperature range of 220 °C to 350 °C, and PDMS mainly undergoing thermal degradation within the range of 350 °C to 570 °C.

The test results are shown in Figure 9. From the graph, it can be observed that the temperature range of 220 °C to 350 °C corresponds to the first stage of silicone rubber thermal decomposition. This stage mainly involves the dehydration and decomposition of the flame retardant ATH, as shown in Figure 10a. The temperature range of 350 °C to 570 °C corresponds to the second stage of thermal decomposition. In this stage, the main degradation process is the cleavage of PDMS, as shown in Figure 10b, producing gases and solid products including methane, ethane, propane, silicon dioxide, carbon monoxide, etc., as shown in Reaction Equation (2). Afterwards, the silicone rubber maintains a stable mass, indicating no further decomposition reactions within the tested temperature range. The TGA test results show that with increasing ageing time, the PDMS content in the silicone rubber sample gradually decreases, indicating a deepening level of corona ageing, which in turn affects the performance of the silicone rubber.

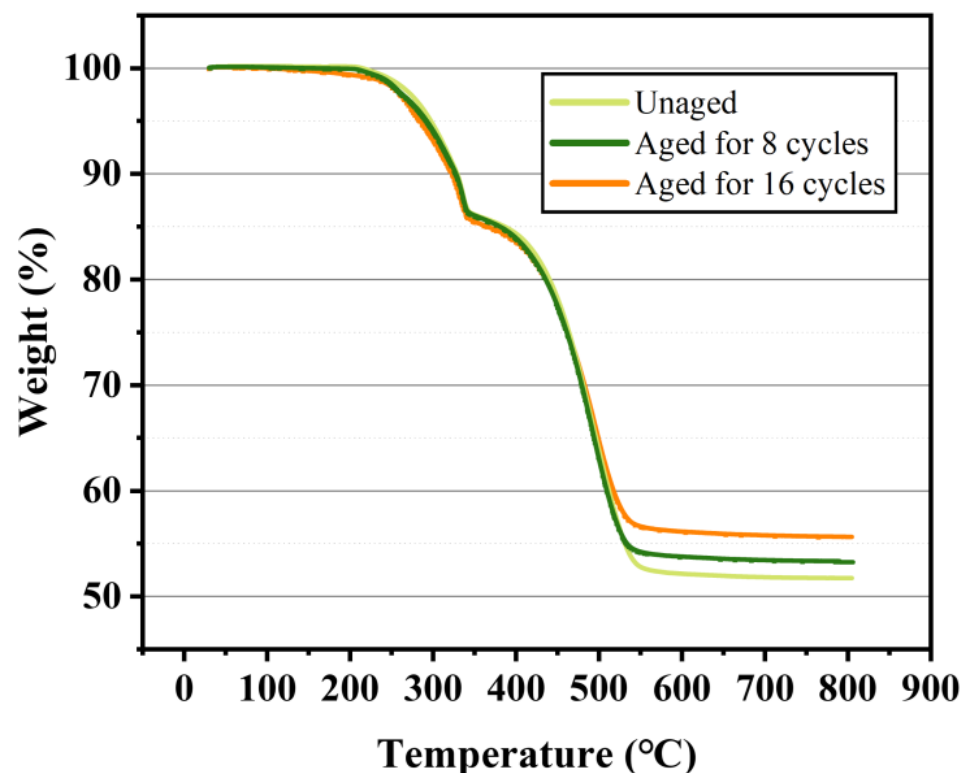


Figure 9. TGA test results of samples with different ageing periods.

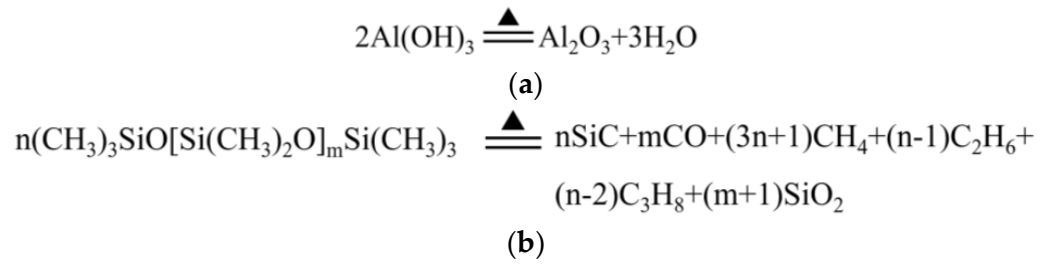


Figure 10. Thermal decomposition reaction equations for silicone rubber. (a) Reaction 1; (b) Reaction 2.

3.4. Moisture Absorption

The moisture absorption weight gain curves for silicone rubber samples at different ageing stages were obtained using Formula (1), as shown in Figure 11.

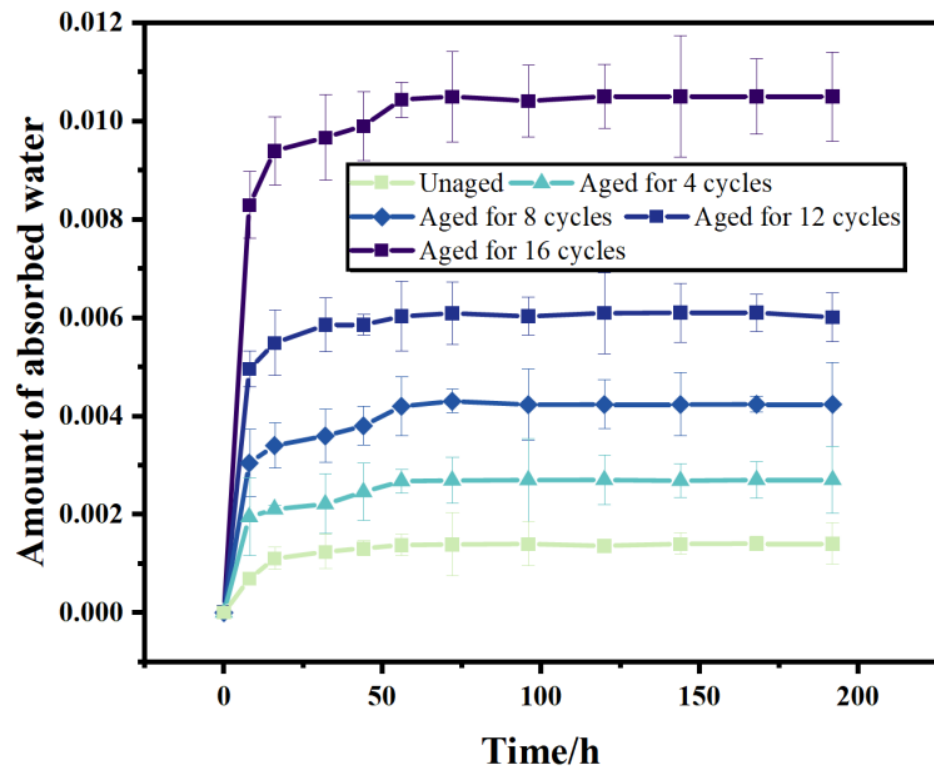


Figure 11. Moisture absorption weight gain curves of silicone rubber samples at different ageing stages.

Currently, there are two main models used to describe the moisture absorption process of composite materials: the Fick diffusion model [27] and the Langmuir diffusion model [28]. The Fick diffusion model assumes that the moisture absorption of composite materials is the result of the random diffusion of water molecules due to their thermal motion. During the absorption process, the mass of the material increases exponentially and gradually approaches saturation. On the other hand, the Langmuir diffusion model considers that besides free diffusion, chemical reactions occur between water molecules and the material during the moisture ingress. It divides the absorption process into two stages—a rapid initial stage with a short duration and a slower second stage with a longer duration—characterized by a distinct inflection point between the two stages. Observing the moisture absorption test curve of silicone rubber materials, it can be inferred that they more closely adhere to the characteristics of the Fick diffusion model.

According to Figure 11, it can be observed that the moisture absorption curve of silicone rubber can be roughly divided into three stages during the test period. In stage I, within the specified time range, the moisture absorption rate of the sample increases linearly with the moisture absorption time. The diffusion behaviour of water is driven by the concentration gradient between the material's interior and the high-humidity environment. In stage II, as the water concentration gradient decreases with increasing moisture absorption time, the moisture absorption rate of the material gradually decreases to zero. The moisture absorption curve in this stage exhibits non-linearity. In stage III, the sample reaches a saturated moisture absorption state, and the moisture absorption rate of the material does not change further, reaching the saturation moisture absorption rate  $M_\infty$ . The expression of the Fick diffusion model is shown in Equation (2), where  $h$  represents the thickness of the silicone rubber sample, and  $D$  represents the moisture diffusion coefficient.

$$\frac{M_t}{M_\infty} = 1 - \frac{8}{\pi^2} \sum_{n=0}^{\infty} \frac{(-1)^n \exp\left\{-\pi^2 t \left[D \left(\frac{2n+1}{h}\right)^2\right]\right\}}{(2n+1)^2} \quad (2)$$

By applying the Fick model's formula and using the least squares method, the moisture absorption test data of samples with different aging periods were fitted, and the diffusion coefficients and fitting degrees of each sample were obtained as shown in Table 4. The fitting degrees of all samples are above 0.95, indicating that the moisture absorption process of the silicone rubber material follows the Fick diffusion model.

**Table 4.** Diffusion coefficients and fitting degrees for different aging stages of silicone rubber material.

Aging Stages of the Samples	Unaged	Aged for 4 Cycles	Aged for 8 Cycles	Aged for 12 Cycles	Aged for 16 Cycles
Diffusion coefficient ( $10^{-3} \text{ cm}^2/\text{h}$ )	1.96	2.68	3.64	5.23	8.19
Fitting coefficient	0.991	0.969	0.972	0.967	0.983

By comparing the diffusion coefficients and saturation moisture absorption of silicone rubber samples at different ageing stages, it can be observed that the saturation moisture absorption rate of silicone rubber gradually increases with the increase in corona ageing time. Combined with SEM and physicochemical analysis results, the reasons can be analyzed as follows: during the corona ageing process, a large amount of energy continuously acts on the PDMS molecular chains, leading to the continuous degradation of long polymer chains. The content of Si–O–Si on the main chain and the Si–CH<sub>3</sub> groups on the side chains decreases, resulting in a deterioration of the hydrophobicity of silicone rubber. At the same time, the surface of the silicone rubber becomes rough, and more and more cracks and pores gradually appear. With the increase in ageing time, these cracks and pores expand into the interior of the material. Water flows and accumulates in these cracks and pores under capillary action, greatly enhancing the moisture absorption performance of the silicone rubber, increasing the diffusion coefficients and saturation moisture absorption.

### 3.5. Dielectric Loss Characteristic

In the high-humidity environment of tropical coastal areas in China, the polarization loss caused by the moisture absorption of aged silicone rubber sheaths under the action of power frequency alternating electric fields is one of the main causes of abnormal heating at the ends of insulators. This study conducted tests on the dielectric loss at different stages of aging, and the results are shown in Figure 12.

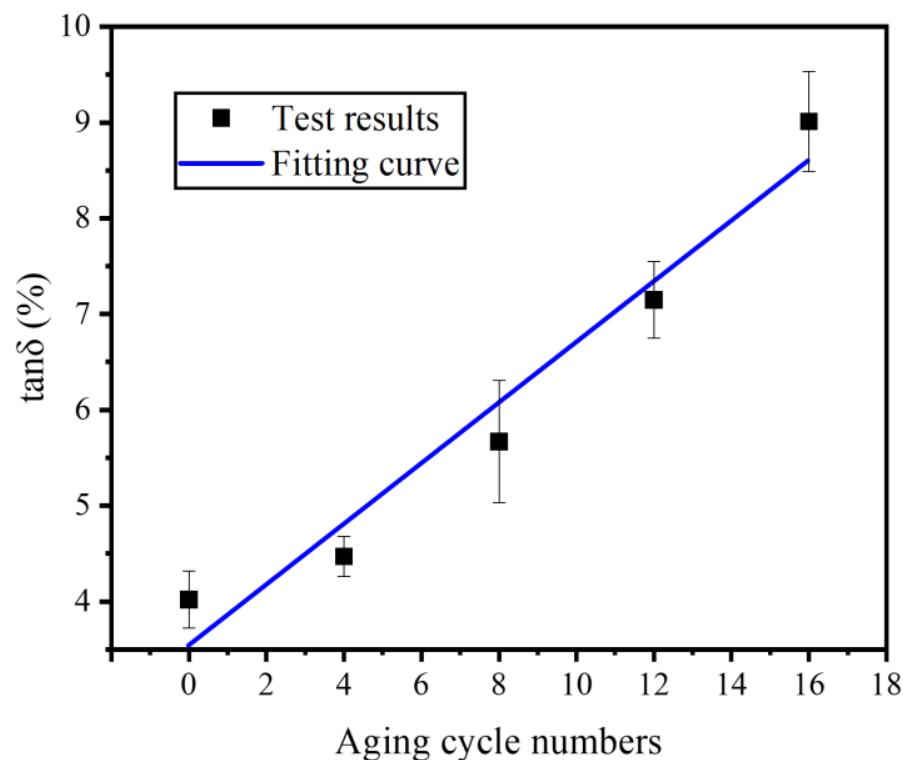


**Figure 12.** The saturated moisture absorption dielectric loss of silicone rubber samples at different ageing stages.

From Figure 12, it can be observed that the dielectric loss of silicone rubber material after saturated moisture absorption gradually increases with ageing time. The Pearson correlation coefficient between the two is 0.979, indicating a strong linear correlation. The increase in the dielectric loss tangent value results in intensified abnormal heating of the composite insulator's sheath at the end, further accelerating the ageing of the sheath.

#### 4. Conclusions

This article established a humidity–heat–electricity–salt spray coupling accelerated ageing test platform to conduct ageing tests on silicone rubber materials used in composite insulators under the combined action of high temperature, high humidity, high salt spray, and high electric field, which are typical factors in tropical coastal areas. The ageing characteristics of silicone rubber materials after multi-factor combined ageing were analyzed using scanning electron microscopy, Fourier infrared spectroscopy, thermogravimetric analysis, and other methods. The main conclusions are as follows.

- (1) Humidity–heat–electricity–salt spray combined ageing can have an impact on the surface morphology of silicone rubber. With increasing ageing time, fillers in silicone rubber continuously precipitate, surface cracks deepen, and deep holes appear in multiple locations, causing further distortion of the local electric field on the silicone rubber surface and accelerating the ageing rate.
- (2) The test results from infrared spectroscopy and thermogravimetric analysis indicate that during the coupled humidity–heat–electricity–salt spray accelerated ageing process of silicone rubber, a significant amount of energy continuously acts on the PDMS molecular chains, leading to the continuous breakdown of long polymer chains and a reduction in the content of Si–O–Si groups on the main chain.
- (3) The main reason for the occurrence of microcavities and micro cracks on the surface of the ageing sheath of silicone rubber materials is the decomposition of PDMS and ATH materials. These micro-defects provide convenient pathways for moisture to intrude into the silicone rubber sheath. In addition, the decrease in the content of



Si–O–Si groups on the PDMS main chain, which is related to the hydrophobicity of the material, leads to a decrease in its hydrophobicity, resulting in a significant increase in the moisture absorption capacity of silicone rubber materials after multi-factor combined ageing, mainly manifested as an increase in the saturation moisture absorption rate. The increased polarizability loss of water molecules in the material, combined with the degradation of the material itself, leads to an increase in the loss tangent value of the saturated moisture absorption medium of silicone rubber. This is the main factor causing abnormal heating of the sheath at the end of composite insulators in tropical coastal areas.

**Author Contributions:** Data curation, J.G. and S.Z.; formal analysis, Y.Z. and Y.L.; funding acquisition, X.L. and L.C.; investigation, X.F. and Y.G.; methodology, X.L., Y.Z. and Y.L.; project administration, X.L.; resources, X.F.; software, L.C.; supervision, L.C.; visualization, Y.Z.; writing—original draft, Y.Z.; writing—review and editing, J.G. All authors have read and agreed to the published version of the manuscript.

**Funding:** This research was funded by the Science and Technology Project of the China Southern Power Grid Co., Ltd. (Canton, China), Grant Number 073006KK62200014, and the APC was funded by China Southern Power Grid Co., Ltd.

**Institutional Review Board Statement:** Not applicable.

**Informed Consent Statement:** Not applicable.

**Data Availability Statement:** Not applicable.

**Conflicts of Interest:** The authors declare no conflict of interest.

## References

1. Shu, Y.; Zhang, W. Research of Key Technologies for UHV Transmission. *Proc. CSEE* **2007**, *31*, 1–6.
2. Zhou, X.; Lu, Z.; Liu, Y.; Chen, S. Development Models and Key Technologies of Future Grid in China. *Proc. CSEE* **2014**, *34*, 4999–5008.
3. Chen, S.; Song, S.; Li, L.; Shen, J. Survey on Smart Grid Technology. *Power Syst. Technol.* **2007**, *31*, 1–6.
4. Zhou, H.; Yu, Y. Discussion on Several Important Problems of Developing UHV AC Transmission in China. *Power Syst. Technol.* **2005**, *29*, 1–9.
5. Cha, M.; Chen, C.; Huang, X.; Wang, Y. Effect of Hainan Climate on Mechanical Properties of RTV Silicone Rubber. *Silicone Mater.* **2015**, *29*, 31–34.
6. Li, T.; Tao, R.; Zhang, R. Infrared Characteristic of Typical Composite Insulator Heating Defects and Selection of Field Unmanned Aerial Vehicle Infrared Test Parameters. *High Volt.* **2022**, *48*, 865–875.
7. Wang, L.; Zhang, Z.; Cheng, L. Effect of Damp Sheath on Abnormal Temperature Rise at End of Composite Insulator. *High Volt.* **2016**, *40*, 608–613.
8. Gong, B. Study on Moisture Absorption Characteristics and Dielectric Properties of Silicone Rubber Material. Master's Thesis, North China Electric Power University, Beijing, China, 2015.
9. Zeng, L. Study on Abnormal Heating and Damp Heat Aging Characteristics of Composite Insulators. Master's Thesis, South China University of Technology, Guangzhou, China, 2019.
10. Liu, S.; Liu, S.; Wang, Q.; Zuo, Z.; Wei, L.; Chen, Z.; Liang, X. Improving surface performance of silicone rubber for composite insulators by multifunctional Nano-coating. *Chem. Eng. J.* **2023**, *451*, 138679. [[CrossRef](#)]
11. Xing, Y.; Wang, Y.; Chi, J.; Liu, H.; Li, J. Study on Improving Interface Performance of HVDC Composite Insulators by Plasma Etching. *Coatings* **2020**, *10*, 1036. [[CrossRef](#)]
12. Wang, J.; Liang, X.; Gao, Y. Failure analysis of decay-like fracture of composite insulator. *IEEE Trans. Dielectr. Electr. Insul.* **2014**, *21*, 2503–2511. [[CrossRef](#)]
13. Liang, X.; Gao, Y.; Wang, J. Rapid Development of Silicone Rubber Composite Insulator in China. *High Volt. Eng.* **2016**, *42*, 2888–2896.
14. Lv, Y.; Zhao, W.; Pang, G. Simulation of Contamination Deposition on Typical Shed Porcelain and Composite Insulators. *Trans. China Electrotech. Soc.* **2018**, *33*, 209–216.
15. Xia, Y.; Song, X.; He, J. Evaluation Method of Aging for Silicone Rubber of Composite Insulator. *Trans. China Electrotech. Soc.* **2019**, *34*, 440–448.
16. Xiong, Y.; Li, Z.; Gong, R. Micro mechanism study on corona aging characteristics of silicone rubber. *Insul. Mater.* **2022**, *55*, 64–70.
17. Cheng, L.; Mei, H.; Wang, L.; Zhang, F.; Dong, H. Study on Long-Term Aging Characteristics and Impact Factors for Silicone Rubber Sheath of Composite Insulators. *Power Syst. Technol.* **2019**, *40*, 1896–1902.

18. Zeng, S.; Li, W.; Peng, Y.; Zhang, Y.; Zhang, G. Mechanism of Accelerated Deterioration of High-Temperature Vulcanized Silicone Rubber under Multi-Factor Aging Tests Considering Temperature Cycling. *Polymers* **2023**, *15*, 3210. [[CrossRef](#)]
19. Zhang, Z.; Qi, J.; Liu, H.; Wang, W.; Zhang, M.; Wu, X. Research on External Insulation Characteristics of Composite Cross-Arm of 10 kV Distribution Network Based on Multi-Factor Aging. *Polymers* **2022**, *14*, 1403. [[CrossRef](#)]
20. Zhang, Z.; Liang, T.; Li, C.; Jiang, X.; Wu, J.; Wu, B. Electrical Strength and Physicochemical Performances of HTV Silicone Rubber under Salt-Fog Environment with DC Energized. *Polymers* **2020**, *12*, 324. [[CrossRef](#)]
21. Liang, Y. Study on the Corona Aging Characteristics and Mechanism of HTV Silicone Rubber. Master's Thesis, North China Electric Power University, Beijing, China, 2008.
22. Wang, Z. Researches on Water Absorptivity and Permeability of Composite Insulator Silicone Rubber and Its Influence Mechanisms. Master's Thesis, Tsinghua University, Beijing, China, 2016.
23. GB/T 2423.17-2008; Environmental Testing for Electric and Electronic Products-Part 2: Test Methods—Test Ka: Salt Mist. China National Standardization Administration: Beijing, China, 2008.
24. ASTM D5229; Standard Test Method for Moisture Absorption Properties and Equilibrium Conditioning of Polymer Matrix Composite Materials. American Society for Testing and Materials: West Conshohocken, PA, USA, 2012.
25. Saidane, E.H.; Scida, D.; Assarar, M.; Ayad, R. Assessment of 3D moisture diffusion parameters on flax/epoxy composites. *Compos. Part A Appl. Sci. Manuf.* **2016**, *80*, 53–60. [[CrossRef](#)]
26. Zhang, Z.; Pang, G.; Lu, M.; Gao, C.; Jiang, X. Research on Silicone Rubber Sheds of Decay-Like Fractured Composite Insulators Based on Hardness, Hydrophobicity, NMR, and FTIR. *Polymers* **2022**, *14*, 3424. [[CrossRef](#)]
27. Boukettaya, S.; Alawar, A.; Almaskari, F.; Ben Daly, H.; Abdala, A.; Chatti, S. Modeling of water diffusion mechanism in polypropylene/date palm fiber composite materials. *J. Compos. Mater.* **2018**, *52*, 2651–2659. [[CrossRef](#)]
28. Roy, S.; Bandorawalla, T. Modeling of diffusion in a micro-cracked composite laminate using approximate solutions. *J. Compos. Mater.* **1999**, *33*, 872–905. [[CrossRef](#)]

**Disclaimer/Publisher's Note:** The statements, opinions and data contained in all publications are solely those of the individual author(s) and contributor(s) and not of MDPI and/or the editor(s). MDPI and/or the editor(s) disclaim responsibility for any injury to people or property resulting from any ideas, methods, instructions or products referred to in the content.